

Spatial-Wideband Effect in Massive MIMO with Application in mmWave Systems

Bolei Wang, Feifei Gao, Shi Jin, Hai Lin, Geoffrey Ye Li, Shu Sun, and Theodore S. Rappaport

To design a practical massive MIMO system, it is important to understand when the spatial-wideband effect appears and how it affects signal transmission, how the spatial-wideband effect interacts with the frequency-wideband effect (frequency selectivity), especially for multi-carrier modulations such as orthogonal frequency-division multiplexing (OFDM), and how we should re-design the transceiver. The authors suggest a new massive MIMO channel model that embraces both the spatial- and frequency-wideband effects.

ABSTRACT

Massive MIMO, especially in the millimeter-wave frequency bands, has been recognized as a promising technique to enhance spectrum and energy efficiency, as well as network coverage for wireless communications. Most research in massive MIMO just uses the extended conventional MIMO channel model by directly assuming that the channel dimensionality becomes large. With massive numbers of antennas, however, there exists a non-negligible propagation delay across the large array aperture, which then causes a transmitted symbol to reach different antennas with different delays, thereby rendering conventional MIMO channel models inapplicable. Such a phenomenon is known as the spatial-wideband effect in the areas of array signal processing and radar signal processing, and introduces the beam squint effect in beamforming. However, the spatial-wideband effect and the related beam squint issue are seldom studied in massive MIMO communications. To design a practical massive MIMO system, it is important to understand when the spatial-wideband effect appears and how it affects signal transmission, how the spatial-wideband effect interacts with the frequency-wideband effect (frequency selectivity), especially for multi-carrier modulations such as orthogonal frequency-division multiplexing (OFDM), and how we should re-design the transceiver. In this article we suggest a new massive MIMO channel model that embraces both the spatial- and frequency-wideband effects, and discuss these issues.

INTRODUCTION

Massive multiple-input and multiple-output (MIMO), also known as large-scale MIMO, is formed by equipping huge numbers of antennas, hundreds or even thousands, at the base station (BS) to simultaneously serve multiple users in the same frequency band. As summarized in [1], massive MIMO can improve spectrum and energy efficiencies, and simple zero-forcing transceivers are asymptotically optimal for the cell throughput and capacity. Furthermore, broadband communications over a millimeter-wave (mmWave) frequency band make massive MIMO attractive since the tiny antenna size facilitates packing a tremendously large number of antennas in a small area [2, 3].

Since channel state information (CSI) is necessary to achieve the huge performance gains for

massive MIMO, various channel estimation algorithms have been designed for uplink channels [4]. Downlink channels for time-division-duplex (TDD) networks can be obtained by channel reciprocity. For frequency-division-duplex (FDD) networks, the angle reciprocity inside uplink/downlink propagation paths can be exploited for downlink channel estimation [5]. With CSI at the BS, various beamforming techniques [6] have been proposed to utilize the high spatial resolution of large-scale arrays. To reduce the cost of hardware implementation, hybrid analog-digital beamforming techniques have been developed for mmWave-band massive MIMO systems, which perform nearly as well as fully digital implementations that become unwieldy when the number of antennas becomes large [7].

In fact, most existing works on massive MIMO directly apply the extended conventional MIMO channel model by simply assuming that the dimensionality of the channel becomes large. However, such a simple extension does not fit the physical reality when the physical size of an antenna array travelled by the propagating wave exceeds a certain level. If this propagation delay across the array is comparable to the symbol period, then different antenna elements will receive different amplitudes and phases of the same symbol or even distinct symbols at the same sampling time, making the conventional MIMO model inapplicable. This is an inherent property of a large-scale array, called the spatial-wideband effect, and it has been extensively investigated in radar signal processing [8]. Unlike narrowband signaling which has a fixed beam with no frequency dependence over the antenna manifold, a wideband signal will have slight variations of the antenna radiation pattern, as a function of frequency, over the wide bandwidth of the signal, which is generally referred to as beam squint [8, 9] deriving from the spatial-wideband effect. Accordingly, a large antenna array is unable to generate beams pointing toward the same directions for different frequencies, and reciprocally, it is difficult to extract the precise incident angles from an incoming signal if the spatial-wideband effect is not carefully considered.

To date, the spatial-wideband effect and the consequent impacts have not yet received much attention in massive MIMO communications, partly due to the fact that most of the existing massive MIMO testbeds are planar arrays and are not massive enough in any single dimension. For example,

the typical 8-by-8 or 16-by-16 planar array testbed, usually with around half wavelength distance between adjacent antennas, is not massive in either dimension and therefore the spatial-wideband effect can hardly be observed. The initial work in [10] considers the spatial-wideband effect when designing a beamspace receiver, where only a line-of-sight (LoS) channel is assumed.

In this article, we investigate wideband massive MIMO communications, taking into account both the spatial-wideband and frequency-wideband effects, called *dual-wideband effects*. For ease of illustration, we consider mmWave-band communications in sparse channel scenarios, which is reasonable from [2]. We model each path of the mmWave massive MIMO channel with the complex gain, the direction of arrival (DoA) or the direction of departure (DoD), and the time delay. We illustrate several characteristics of dual-wideband channels and how to design orthogonal frequency division multiplexing (OFDM) to embrace the dual-wideband effects. We also compare the performance of channel estimation between ignoring and considering the spatial-wideband effect, where the approaches neglecting the spatial-wideband effect suffer from severe performance degradation in broadband transmission. This article concludes with a discussion of how the transceiver architecture should be re-designed for massive MIMO systems undergoing dual-wideband effects.

Spatial-Wideband Effect in Massive MIMO

The spatial-wideband effect in a large antenna array, in essence, is similar to the frequency-wideband effect (frequency selectivity). While frequency selectivity results from multipath delay, the spatial-wideband effect exists on a large antenna array even in an LoS channel with no multipath. In this section, we first introduce the principle of the spatial-wideband effect and then derive the *dual-wideband channel model*. Next, several characteristics related to the dual-wideband effects are discussed for massive MIMO OFDM systems, which can be leveraged for user scheduling as discussed below.

Spatial-Wideband Effect

The spatial-wideband effect, induced by the physical propagation delay of the electromagnetic wave traveling across the antenna aperture, occurs in high-dimensional arrays, as shown in Fig. 1. Consider one signal from a far-field source impinging upon a uniform linear array (ULA) of M antenna elements with the single DoA ϑ . According to the Huygens-Fresnel wave propagation principle, the received signals at different antenna elements are slightly delayed versions of the original signal, unless the incident signal is perpendicular to the ULA. The time differences at different antenna elements compared to the first one form an arithmetic progression with common difference determined by the path DoA and the element spacing of the antenna array.

To better demonstrate the impact of the spatial-wideband effect, we first use single-carrier modulation as an example in Fig. 1. If the number of antenna elements is small, then the propagation delay across the overall array is much small-

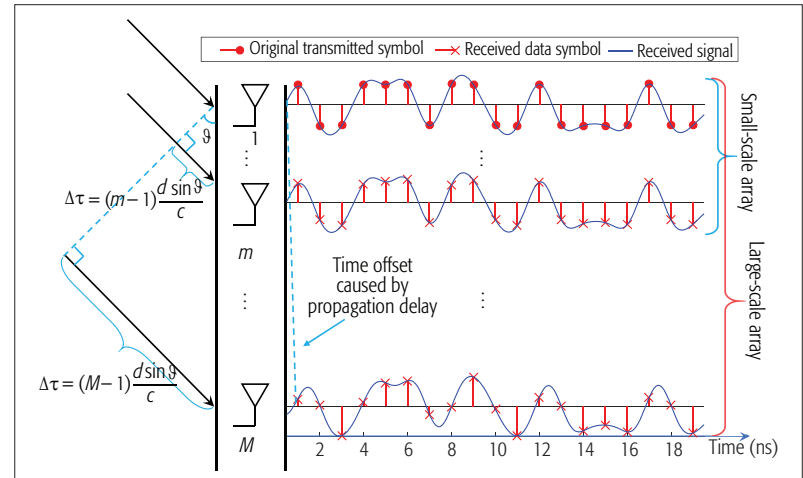


Figure 1. An illustration of the spatial-wideband effect in a ULA.

er compared to the symbol period and can be ignored. In this case, the received symbols at different antenna elements can be viewed as from the identical symbol series and the conventional MIMO channel model is applicable. In general, this is true only when the maximum propagation delay is much less than the symbol period.

When the number of antenna elements in the array is large, the propagation delay becomes a significant fraction of the symbol period or even more than one symbol period. In this case, the amplitudes and phases of the received symbols at different antenna elements at the same time will be different. As a result, the conventional MIMO channel model, which ignores the delay differences among the received signals from different antenna elements, does not hold for a practical antenna array.

For example, for a ULA system with 128 antenna elements and half wavelength antenna element spacing, the maximum propagation delay will be $0.489 T_s$ in a typical LTE system with the transmission bandwidth of 20 MHz at the carrier frequency 2.6 GHz, where T_s denotes the symbol period. In a typical mmWave-band system with a bandwidth of 1 GHz at 60 GHz carrier frequency, such delay will be $1.058 T_s$. This 60 GHz example shows that the last antenna element sees a completely different symbol from the first one in a large-scale array, which makes the conventional MIMO channel model invalid.

It should be noted that the spatial-wideband effect exists not only in ULAs, but in any array topology where the large aperture causes non-negligible propagation delay compared with the symbol duration. A typical instance is the base station of Facebook Project Aries, where a 48-by-2 planar array for the centimeter-wave frequency band is employed and the spatial-wideband effect plays an important role in the 48-element dimension. Another typical instance is in phased-array radars. For example, the AN/TPY-2 wideband radar operating at approximately 10 GHz contains 25,344 antenna elements in the 9.2 m^2 area, where the spatial-wideband effect appears in both dimensions.

Despite the single-carrier modulation used in the above example, the conclusion could also be true under some conditions for multi-carrier modulations, such as for OFDM systems.

With the spatial-wideband effect, each path forms a square region instead of a narrow impulse in angular-delay domain. Two multipath channels are orthogonal as long as they do not share the same path, which is called the angular-delay orthogonality.

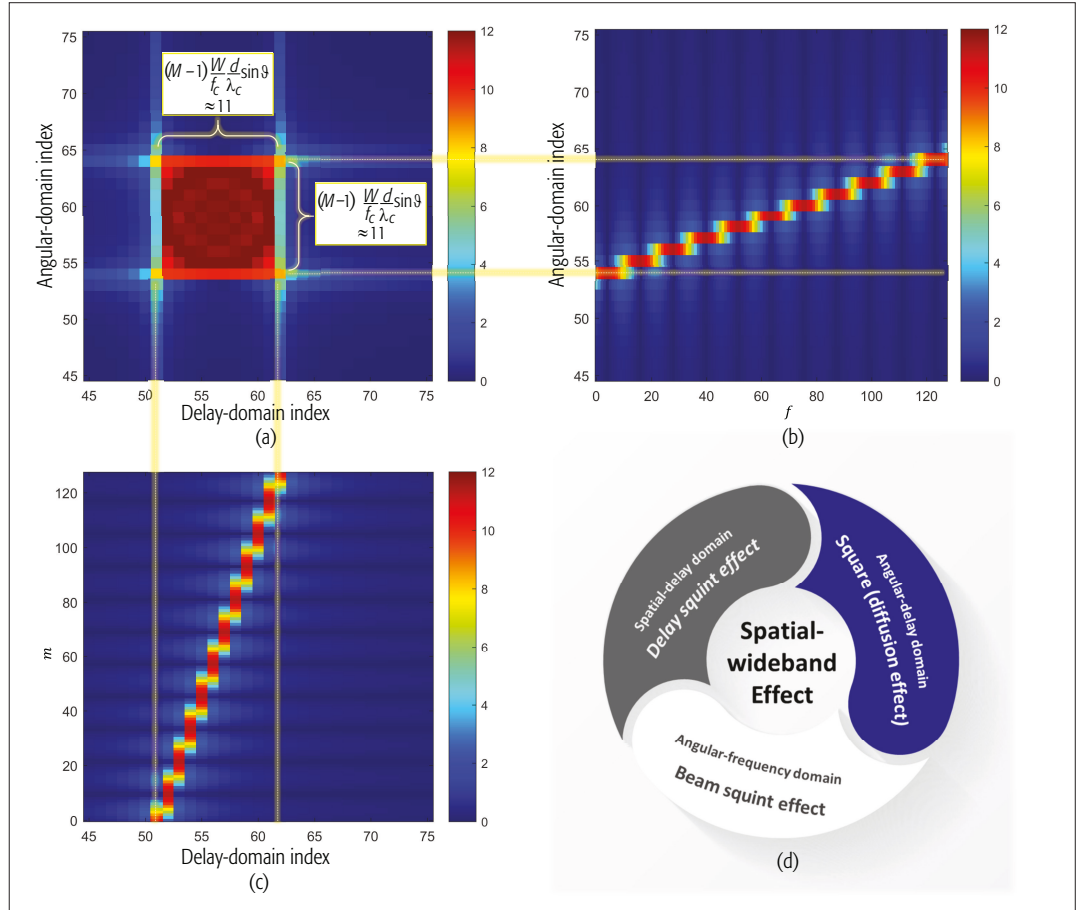


Figure 2. SFW channel in different domains: a,b,c) a one-path SFW channel in angular-delay domain, angular-frequency domain, and spatial-delay domain, respectively; d) manifestations of spatial-wideband effect in different domains.

DUAL-WIDEBAND CHANNEL

From the above discussion, the spatial-wideband effect cannot be ignored for massive MIMO systems. We need to revise the conventional MIMO channel model by taking the delay differences among antennas into consideration.

Let us consider a massive MIMO system consisting of one BS with an M -antenna ULA and a single-antenna user. For ease of illustration, we consider mmWave-band transmission. Suppose that there are L individual physical paths between the BS and the user.¹ Denote ϑ_l as the DoA of the l th path and $\tau_{l,m}$ as the time delay of the l th path from the user to the m th antenna. Then, the uplink channel in the time domain at the m th antenna can be modeled as

$$h_m(t) = \sum_{l=1}^L \alpha_l e^{-j2\pi(m-1)\frac{d\sin\vartheta_l}{\lambda_c}} \delta(t - \tau_{l,m}), \quad (1)$$

where α_l is the complex channel gain of the l th path, ϑ_l is the DoA of the l th arriving path, and λ_c is the carrier wavelength.

For a traditional small-scale MIMO system, the time delay of a path at different antennas can be regarded as the same. Therefore, Eq. 1 could be compactly organized by the well known spatial-domain steering vector $\mathbf{a}(\vartheta_l)$, which, however, cannot be cloned when the spatial-wideband effect must be considered. To obtain a more compact form of the dual-wideband massive

MIMO channel, let us investigate it in the frequency domain.

Suppose we have N equal-spaced sub-bands, for example, N subcarriers in OFDM modulation. By transforming the time-domain channel (1) into the frequency domain and utilizing the arithmetic progression of time delays at different antenna elements across the array aperture, the overall spatial-frequency channel matrix from all M antennas can be represented as [11]

$$\mathbf{H} = \sum_{l=1}^L \alpha_l \left(\mathbf{a}(\vartheta_l) \mathbf{b}^T(\tau_{l,1}) \right) \circ \Theta(\vartheta_l) \in \mathbb{C}^{M \times N}, \quad (2)$$

where “ \circ ” denotes the Hadamard product, $\mathbf{b}(\tau_{l,1})$ is the “frequency-domain steering vector” pointing toward the delay of the l th path, and the M -by- N matrix $\Theta(\vartheta_l)$ provides the additional phase shifts to express the effect of the spatial-wideband effect, which is dependent on the DoA and the orientation of the array. Equation 2 provides an exact channel model for large-scale antenna arrays and is called the spatial-frequency wideband (SFW) channel.²

Actually, when the spatial-wideband effect is negligible as in a conventional MIMO channel, the Hadamard factor $\Theta(\vartheta_l)$ in Eq. 2 degenerates into an all-ones matrix, or equivalently disappears. In this conventional case, the spatial-frequency channel can be completely described by the spatial-domain and frequency-domain steering vectors.

¹The extension to low frequency-band communications can be made by integrating within the angular spread caused by local scattering.

²If a uniform planar array (UPA) is applied, then Eq. 2 can be straightforwardly modified with tensor representation.

SFW CHANNEL IN DIFFERENT DOMAINS

Note that Eq. 2 expresses the SFW channel in the spatial-frequency domain. We can transform Eq. 2 to other domains via the discrete Fourier transform (DFT) or the inverse DFT (IDFT) to gain more physical insights.

Let us consider an SFW channel \mathbf{H} consisting of one path with the DoA of 57° as an example.³ By applying IDFT in the spatial domain and/or the frequency domain, we can transform \mathbf{H} into the angular-frequency domain channel matrix, $\mathbf{F}_M^H \mathbf{H}$, the spatial-delay domain channel matrix, $\mathbf{H} \mathbf{F}_N^H$, and the angular-delay domain channel matrix, $\mathbf{F}_M^H \mathbf{H} \mathbf{F}_N^H$, as in Figs. 2b, 2c, and 2a, respectively, where \mathbf{F}_M and \mathbf{F}_N denote the normalized DFT matrix with dimensions M and N , respectively. After the transform, the physical DoA or DoD is mapped from the continuous interval $[-(\pi/2), \pi/2]$ to the set of integers $[0, M-1]$ (angular-domain indices) while the path delay is mapped from the continuous interval $[0, NT_s]$ to the set of integers $[0, N-1]$ (delay-domain indices).

Figure 2c shows the path delay versus the antenna index (spatial domain). From this figure, different antennas “see” the sequences of distinct delays, which we call the *delay squint* effect. Correspondingly, different frequency sub-bands “see” the distinct “angles” as illustrated in Fig. 2b, which is called the *beam squint* in array signal processing theory [12]. With the beam and the delay squints, the square region in Fig. 2a represents the single path in the angular-delay domain.

Without the spatial-wideband effect, the Hadamard factor in Eq. 2, $\theta(\cdot)$, does not exist and each path manifests an impulse in the angular-delay domain. With the spatial-wideband effect, $\theta(\cdot)$ diffuses the energy of each path from an impulse to a square region, which we call the *diffusion effect*.

We have shown in [11] that the diffusion region corresponding to each path will converge to a square asymptotically as the number of antennas and that of frequency sub-bands tend to infinity and the size of the square will be the exact ratio of maximum propagation delay across the whole antenna to the time-domain sample period. Moreover, the squints of angle and delay in Figs. 2b and 2c can be proved to be identical, each being the side length of the square or equivalently the propagation delay of each path in time-domain samples. In the given example, the path with the DoA of 57° travels across the array in 11 time-domain samples and forms a square with the side length of 11.

The above three manifestations of the spatial-wideband effect can be summarized in Fig. 2d. Traditionally, large arrays are mainly applied in radar systems. Due to the impact of beam squint, a phased-array radar radiates the dispersed beam with different frequency components pointing toward different directions. This severe and evident performance loss in wideband beamforming [12] has motivated studies on the spatial-wideband effect in radar signal processing. In contrast, as conventional wireless communication systems mainly apply the small-scale MIMO, the spatial-wideband effect can be easily ignored and therefore has not been explored much.

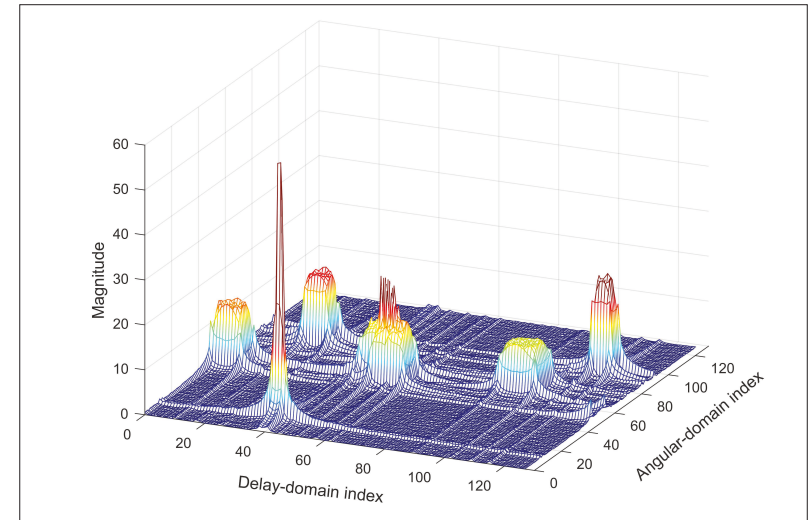


Figure 3. A multipath SFW channel in angular-delay domain.

ANGULAR-DELAY ORTHOGONALITY

In this subsection, we discuss the orthogonality of the SFW channels. Two channels are defined to be orthogonal if the dot product of their vectorized versions of spatial-frequency channel matrices equals zero.

Without the spatial-wideband effect, each path forms a narrow impulse in the angular-delay domain. In this case, as long as two multipath channels do not share the same path,⁴ these two channels are asymptotically orthogonal to each other [4], which is called the *angular-delay orthogonality*.

With the spatial-wideband effect, each path forms a square region in the angular-delay domain due to the diffusion effect, possibly with distinct sizes related to the different propagation delays from different DoAs. Figure 3 demonstrates an example of a multipath SFW channel in the angular-delay domain. Unlike the narrow impulses in the frequency-wideband-only scenario, two distinct paths may overlap with each other in the angular-delay domain, which, however, does not break the angular-delay orthogonality. In particular, two single-path SFW channels, with partial overlaps in the angular-delay domain, are still asymptotically orthogonal to each other from [11].

Therefore, for users at different locations or for users at the same location but with different path delays, the BS can distinguish them and separate their signals by filtering in the angular-delay domain, which makes it possible to communicate with them simultaneously without inter-user interference. The angular-delay orthogonality continues to play an important role with dual-wideband effects in user scheduling in massive MIMO systems.

CYCLED PREFIX IN MASSIVE MIMO OFDM SYSTEMS

In this subsection, we focus on the impact of dual-wideband effects on massive MIMO OFDM systems.

Figure 4 illustrates how dual-wideband effects demand minimal cyclic prefix (CP), where $B[i]$ and $B_{CP}[i]$ denote the i th time-domain OFDM block and the corresponding CP. For a single antenna as shown in Fig. 4a, the length of CP

³ To illustrate the characteristics clearer, the ratio of the transmission bandwidth to the carrier frequency is set 0.2, much higher than real systems such that the sizes of squares are magnified.

⁴ Two paths are defined identical if they have both the same DoA and the same path delay.

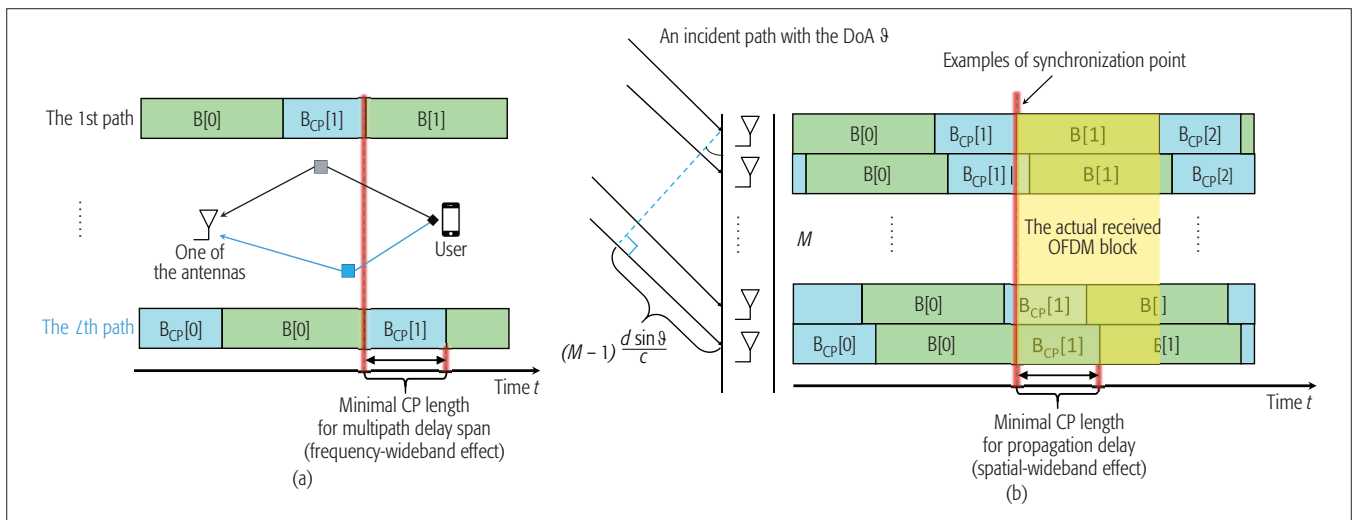


Figure 4. Dual-wideband effects in a massive MIMO OFDM system, where $B[i]$ and $B_{CP}[i]$ denote the i th OFDM block and the corresponding CP: a) the traditional CP for multipath delay span and b) the additional CP for propagation delay.

is at least the delay span, that is, the time difference of the maximum and the minimum delays caused by the multiple paths. For the overall array as shown in Fig. 4b, an extra CP is necessary to address the propagation delay due to the spatial-wideband effect; otherwise, inter-block interference would be introduced. Thus, the CP for the spatial-wideband effect should be at least the propagation delay across the array, as marked by the interval between the two vertical lines in Fig. 4b.

Denote τ_l as the multipath delay observed by any one of the antennas. By combining the two parts of CP respectively shown in Figs. 4a and 4b, the required CP in the number of time-domain samples in the dual-wideband scenario can be expressed as [11]

$$(M-1) \frac{W}{f_c} \frac{d}{\lambda_c} + W \max_l \tau_l \frac{d = \lambda_c/2}{2} \frac{M-1}{f_c} W + W \max_l \tau_l, \quad (3)$$

where the first term is the maximum propagation delay caused by the spatial-wideband effect and the second term is the exact multipath delay span.

For the typical mmWave-band system with the bandwidth of 1 GHz at 60 GHz carrier frequency, the CP length exclusively induced by the spatial-wideband effect is 2 and 5 for the 128-antenna and the 512-antenna ULAs, respectively. Hence the CP for the spatial-wideband effect in large-scale antennas seems not to be a big burden for the existing OFDM protocols. Nevertheless, the subsequent numerical results demonstrate that the spatial-wideband effect must be considered. Even equipped with sufficient CP, the existing algorithms without considering spatial-wideband effect still suffer from severe performance loss in OFDM systems.

It needs to be mentioned that even for the flat-fading or LoS environments, the first term in Eq. 3 is still non-zero due to the spatial-wideband effect. In this case, adding CP and performing OFDM may still be required, which is different from the conventional techniques for flat fading.

RETHINKING CHANNEL ESTIMATION AND DATA TRANSMISSION

In this section, we discuss when the spatial-wideband effect will appear and how it will affect channel estimation and data transmission.

Consider a massive MIMO OFDM system consisting of a BS with a large-scale ULA and 10 single-antenna users that are randomly distributed in the coverage area. The carrier frequency is set as 60 GHz and the antenna spacing of the ULA is the half wavelength. The dual-wideband channel estimation algorithm [11] and the conventional frequency-wideband-only algorithm [13] are compared in Fig. 5 in terms of the normalized mean-square error (NMSE).

Figure 5 demonstrates the NMSE of channel estimation versus the number of antennas under different SNRs and signal bandwidths. For a system with bandwidth of 1 GHz, the spatial-wideband effect becomes obvious as the number of antennas is 16, corresponding to the maximum propagation delay of 0.13Ts. Such a delay is not significant compared to one sample period but starts to deteriorate the frequency-wideband-only channel estimation approach. When the number of antennas in a ULA is 16 or smaller, it is not necessary to consider the spatial-wideband effect, which explains why the current massive MIMO prototypes based on an 8-by-8 planar array or 16-by-16 planar array do not observe the spatial-wideband effect because their one-side dimensionality is not “massive” enough if the distance between adjacent antennas is around a half wavelength. For a system with the transmission bandwidth of 0.25 GHz, the sample period is longer and Fig. 5 shows that the spatial-wideband effect is not evident when the number of antennas in a ULA is fewer than 48.

It needs to be noted that all the above examples have provided the sufficient CP length for both the dual-wideband algorithm and the frequency-wideband-only approach, but the latter still suffers from performance loss due to the spatial-wideband effect. It can be concluded that for a massive MIMO system with the propagation delay comparable to or larger than 0.1Ts, the

spatial-wideband effect is evident and should be properly treated.

CHALLENGES ON TRANSCEIVER DESIGN

For mmWave-band communications, the channel is sparse in angle and delay domains. A ULA with half-wavelength antenna spacing is usually applied to avoid the ambiguity in the angle domain for both channel estimation and beamforming. Since the spatial-wideband effect distracts the direction of beamforming due to beam squint, how to design the transceivers to avoid the effect of beam squint will be an interesting problem. In terms of distinct hardware costs and implementation complexities, there are generally three typical architectures: analog beamforming, digital precoding and combining, and hybrid analog/digital precoding and combining.

ANALOG BEAMFORMING

The analog beamforming transceiver usually comprises only one radio frequency (RF) chain connecting between the exclusive baseband processing module and multiple antenna elements, each of which is fed by a phase shifter. Generally, a power divider inside the antenna controls all phases and amplitudes. The divider, known as a fixed Butler Matrix, is a passive device. Thus, the number of beams, the corresponding beamforming angles, and sidelobes cannot be changed after installation. This configuration is often referred to as a switched-beam antenna array or passive antenna array. As hardware has been evolving, active beamforming antennas have been developed to separately control the phase of each array element, and enable the beam to be steered to virtually any angle rather than to discrete angles [12].

For its superiority in low hardware cost and low implementation complexity, the analog beamforming architecture is widely used at present though the hardware constraints in a Butler Matrix and only one RF chain limit it to single-stream transmission [7]. Nevertheless, the spatial-wideband effect in massive MIMO configurations causes analog beamforming to suffer from severe performance loss if not properly handled. Since a phase shifter could only provide the identical phase shift to a signal under different frequency bands, it is unable to deal with the beam squint effect caused by the spatial-wideband effect, which requires the frequency-dependent phase shift of a transmitted signal. An algorithm to compensate for the beam squint has been developed in [9] by increasing the codebook size in precoding, whereas it has also been proved that phased-array beamforming cannot solve the beam squint problem when either the transmission bandwidth or the number of antennas becomes large.

If the receiver processes the received signal in the time domain, then the propagation delay among antennas can be compensated by delay lines instead of phased shifters. Delay lines compensate the delays of different antennas in the time domain and naturally produce frequency-dependent phase shift. Such a configuration is referred to as true-time-delay (TTD) beamforming [14], which has been used in high-bandwidth radars and ultra-wideband (UWB) multi-antenna systems. However, TTD systems increase the

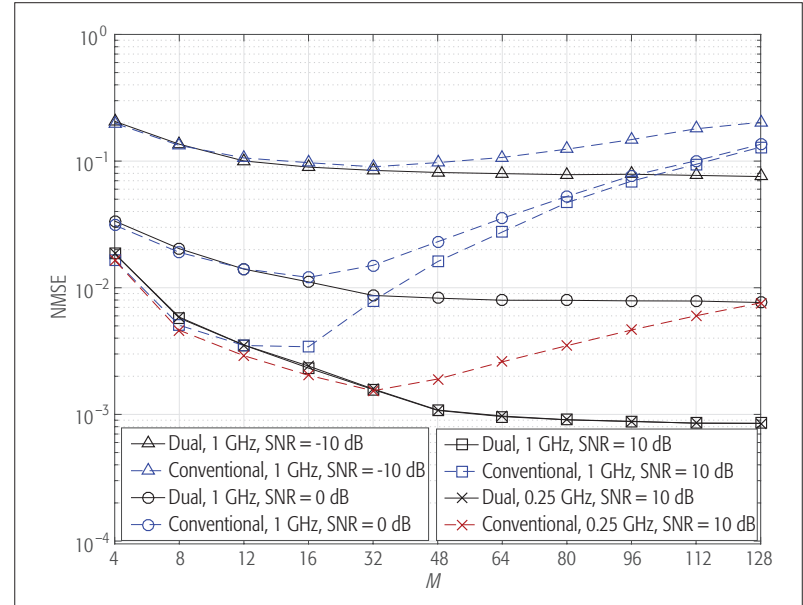


Figure 5. Downlink performance comparison between the proposed method and the compressive sensing-based frequency-wideband-only approach under different SNRs and bandwidths.

hardware complexity and limit the transmission rate. How to deal with the spatial-wideband effect in analog beamforming systems remains to be studied.

DIGITAL PRECODING AND COMBINING

The digital precoding and combining transceiver consists of multiple digital baseband processing modules and the same amounts of RF chains, each connecting to an antenna. Thus, it has the highest flexibility and offers very good performance. By carefully designing digital baseband processing modules [11], the dual-wideband effects can be well managed. It should be noted that the full-digital architecture results in very high hardware costs, significantly increases energy consumption, and complicates integration in mobile devices [12]. It is an interesting issue how to find a proper structure to balance performance and complexity.

As the hardware cost of high-resolution analog-to-digital converters (ADCs) is high, applying low-resolution ADCs in RF chains can significantly reduce cost and the energy consumption. Without the spatial-wideband effect, massive MIMO-based spatial oversampling helps low-resolution ADCs decode the received symbols. With the spatial-wideband effect, different antennas at each sampling time collect non-identical data symbols or the same symbol with pulse shaping waveform-related magnitudes, which makes it harder to correctly decode by the spatial oversampling. Decoding with the spatial-wideband effect under low-resolution ADCs is still an open problem.

HYBRID ANALOG/DIGITAL PRECODING AND COMBINING

Hybrid analog/digital precoding and combining architecture has fewer digital baseband processing modules and RF chains than the number of antennas. It has the advantages of both analog and digital structures.

Even if there are many different hybrid array configurations, each RF chain is linked with mul-

Operation	Issues
Channel estimation, user scheduling	Changes of effective channel parameters due to angular-delay diffusion
Inter-antenna synchronization	Uncompensable delay squint
Analog (hybrid) beamforming/combining, sidelobe control	Beam squint
Low-resolution ADCs	Complicated decoding process

Table 1. Challenges and issues with dual-wideband effects.

multiple antennas, and thus the corresponding disadvantages of analog beamforming still exist. Since the phase shifters cannot handle the spatial-wideband effect, an elaborate codebook design similar to [9] in analog beamforming might be required to compensate for part of the beam squint. It has been discovered in [15] that the performance of the phased-array hybrid structure will degrade as the bandwidth increases. The analog tapped delay lines could be applied to substitute the phase shifters and handle the spatial-wideband effect, but incur much higher complexity. The switch-based hybrid architecture, which uses on/off switches to replace phase shifters or delay lines, might be a good choice.

Nevertheless, most existing studies of hybrid precoding and combining are still based on the extended conventional MIMO channel model, where the spatial-wideband effect is overlooked. Moreover, in frequency-domain scheduling, such as the existing OFDMA, users are served on different subcarriers, and the large bandwidth across subcarriers will induce the evident beam squint, making the existing narrowband hybrid precoders no longer applicable. Therefore, how to deal with both the spatial-wideband and frequency-wideband effects in hybrid architectures is still an open issue. Table 1 summarizes the challenges and issues due to the spatial-wideband effect.

CONCLUSIONS

In this article, we discussed the spatial-wideband effect for wideband massive MIMO communications that arises from the non-negligible propagation delay across a large-scale antenna array. It has been shown that the large-scale array aperture and the large transmission bandwidth will cause the spatial-wideband effect. The existing channel estimation algorithms only consider the frequency-wideband effect and suffer from performance loss. We have analytically presented a new channel model that takes the dual-wideband effect into consideration. Moreover, we have modified OFDM design to cope with the dual-wideband effects. In general, various transceiver algorithms need to be re-designed due to the spatial-wideband effect and beam squint, leaving many open issues in massive MIMO communications.

ACKNOWLEDGMENT

This work was supported in part by the National Natural Science Foundation of China under Grant 61771274 and the Beijing Natural Science Foundation under Grant 4182030. The work of S. Jin was supported in part by the National Natural Science Foundation of China under Grant

61531011. The work of H. Lin was supported by JSPS KAKENHI Grant Number 17K06435.

REFERENCES

- [1] L. Lu et al., "An Overview of Massive MIMO: Benefits and Challenges," *IEEE J. Sel. Topics Signal Process.*, vol. 8, no. 5, Oct. 2014, pp. 742–58.
- [2] J. Lota et al., "5G Uniform Linear Arrays with Beamforming and Spatial Multiplexing at 28, 37, 64, and 71 GHz for Outdoor Urban Communication: A Two-Level Approach," *IEEE Trans. Veh. Technol.*, vol. 66, no. 11, Nov. 2017, pp. 9972–85.
- [3] I. Hemadeth et al., "Millimeter-Wave Communications: Physical Channel Models, Design Considerations, Antenna Constructions and Link-Budget," *IEEE Commun. Surveys Tuts.*, vol. 20, no. 2, 2018, pp. 870–913.
- [4] Z. Chen and C. Yang, "Pilot Decontamination in Wideband Massive MIMO Systems by Exploiting Channel Sparsity," *IEEE Trans. Wireless Commun.*, vol. 15, no. 7, Jul. 2016, pp. 5087–5100.
- [5] H. Xie et al., "A Unified Transmission Strategy for TDD/FDD Massive MIMO Systems with Spatial Basis Expansion Model," *IEEE Trans. Veh. Technol.*, vol. 66, no. 4, Apr. 2017, pp. 3170–84.
- [6] A. Adhikary et al., "Joint Spatial Division and Multiplexing for mm-Wave Channels," *IEEE JSAC*, vol. 32, no. 6, Jun. 2014, pp. 1239–55.
- [7] A. Alkhateeb et al., "MIMO Precoding and Combining Solutions for Millimeterwave Systems," *IEEE Commun. Mag.*, vol. 52, no. 12, Dec. 2014, pp. 122–31.
- [8] W. Liu and S. Weiss, *Wideband Beamforming: Concepts and Techniques*, John Wiley & Sons, 2010.
- [9] M. Cai et al., "Effect of Wideband Beam Squint on Codebook Design in Phased-Array Wireless Systems," *Proc. 2016 IEEE Glob. Commun. Conf. (GLOBECOM)*, Washington, DC, 2016, pp. 1–6.
- [10] J. H. Brady and A. M. Sayeed, "Wideband Communication with High-Dimensional Arrays: New Results and Transceiver Architectures," *Proc. 2015 IEEE Int'l. Conf. Commun. Workshop (ICCW)*, London, 2015, pp. 1042–47.
- [11] B. Wang et al., "Spatial- and Frequency-Wideband Effects in Millimeter-Wave Massive MIMO Systems," *IEEE Trans. Signal Process.*, vol. 66, no. 13, Jul. 2018, pp. 3393–3406.
- [12] M. Reil and G. Lloyd, *Millimeter-Wave Beamforming: Antenna Array Design Choices & Characterization*, Rohde & Schwarz, Oct. 2016; available: <http://www.rohde-schwarz.com/appnote/1MA276>, accessed Oct. 28, 2016.
- [13] J. Fang et al., "Super-Resolution Compressed Sensing for Line Spectral Estimation: An Iterative Reweighted Approach," *IEEE Trans. Signal Process.*, vol. 64, no. 18, Sept. 2016, pp. 4649–62.
- [14] H. Hashemi, T. Chu, and J. Roderick, "Integrated True-Time-Delay-Based Ultra-Wideband Array Processing," *IEEE Commun. Mag.*, vol. 46, no. 9, Sept. 2008, pp. 162–72.
- [15] J. A. Zhang et al., "Massive Hybrid Antenna Array for Millimeter-Wave Cellular Communications," *IEEE Wireless Commun.*, vol. 22, no. 1, Feb. 2015, pp. 79–87.

BIOGRAPHIES

BOLEI WANG [S'15] received the B.Eng. degree in electrical engineering from the University of Electronic Science and Technology of China (UESTC), Chengdu, China, in 2015. He is working toward the Ph.D. degree at Tsinghua National Laboratory for Information Science and Technology (TNList), Tsinghua University, Beijing, China. His current research interests include signal processing for communications and broadband wireless communications, with a focus on massive MIMO systems and millimeter-wave communications.

FEIFEI GAO [M'09, SM'14] is an associate professor with the Department of Automation, Tsinghua University, Beijing, China. His research areas include communication theory, signal processing for communications, array signal processing, and convex optimizations. He has authored/coauthored more than 100 refereed IEEE journal papers and more than 100 IEEE conference proceeding papers, which have been cited more than 5000 times from Google Scholar.

SHI JIN [S'06, M'07, SM'17] is currently with the faculty of the National Mobile Communications Research Laboratory, Southeast University. His research interests include space time wireless communications, random matrix theory, and information theory. He and his co-authors have been awarded the 2011 IEEE Communications Society Stephen O. Rice Prize Paper Award in the field of communication theory and the 2010 Young Author Best Paper Award by the IEEE Signal Processing Society.

HAI LIN [M'05, SM'12] received the Dr. Eng. degree from Osaka Prefecture University, Japan, in 2005. Since 2000, he has been a research associate in the Graduate School of Engineering, Osaka Prefecture University, where he is now an associate professor. He has been an editor of *IEEE Transactions on Wireless Communications*, and he is currently an editor of *IEEE Transactions on Vehicular Technology*. His research interests are in signal processing for communications, wireless communications, and statistical signal processing.

GEOFFREY LI is a professor with Georgia Tech. His general research is in signal processing and machine learning for wireless communications. In related areas, he has published over 400 articles with over 30,000 citations and been listed as a Highly-Cited Researcher by Thomson Reuters. He is an IEEE Fellow. He has won several awards from the IEEE Communications Society, IEEE Signal Processing Society, and IEEE Vehicular Technology Society, and a Distinguished ECE Faculty Achievement Award from Georgia Tech.

SHU SUN [S'13] received her B.S. degree in applied physics from Shanghai Jiao Tong University in 2012, her M.S. degree in electrical engineering from NYU Tandon School of Engineering in 2014, and her Ph.D. degree from NYU in 2018. She is a recipient of the 2017 Marconi Society Paul Baran Young Scholar Award. She has over 40 papers in the field of mmWave wireless communications, including three IEEE award-winning papers.

THEODORE (TED) S. RAPPAPORT is the David Lee/Ernst Weber Professor of Electrical Engineering at NYU's Tandon School of Engineering, as well as a Professor of Computer Science at NYU's Courant Institute and a Professor of Radiology at NYU's School of Medicine. He founded NYU WIRELESS in 2012, and founded academic wireless research programs at The University of Texas at Austin and Virginia Tech earlier in his career. His work proved the viability of millimeter wave mobile communications.